ELSEVIER

Journal of Molecular Structure (Theochem) 686 (2004) 65–70

THEO CHEM

www.elsevier.com/locate/theochem

A theoretical study of the ion pair S_N2 reaction between lithium isocyanates with methyl fluoride with inversion and retention mechanism

Hua-jie Zhu[a], Yi Ren[b,*], Jie Ren[a]

[a]*State Key Lab of Phytochemistry and Plant Resources in West China, CAS, Kunming 650200, People's Republic of China*
[b]*College of Chemistry, Sichuan University, Faculty of Chemistry, P.O. Box No. 73, Chengdu 610064, People's Republic of China*

Received 5 April 2004; revised 20 August 2004; accepted 20 August 2004

Abstract

This paper is devoted to a detailed theoretical study of an ion pair S_N2 reaction $LiNCO + CH_3F$ in the gas phase and in solution at the level of MP2(full)/6-31+G**//HF/6-31+G**. Two possible reaction mechanisms, inversion and retention, are discussed. There are eight possible reaction pathways. The inversion mechanism is more favorable no matter in the gas phase or in solution based on analyses of the transition structures. Methyl isocyanate should form preferentially in the gas phase and more stable methyl cyanate is the main product in solution. The retardation of the reaction in solvents was attributed to the difference in solvation in the separated reactants and in the transition state.

Keywords: Cyanate and isocyanate; Ion pair S_N2 reaction; Ab initio; Inversion and retention mechanism

1. Introduction

Molecules with an ambidextrous cyanate group –OCN are very reactive compounds and widely used in organic, bioorganic chemistry, and industry because the cyanate group is able to react at the site of either the oxygen or nitrogen atom, forming cyanates R-OCN or their isomers—isocyanates, R-NCO [1]. Unlike their thio derivatives, there have been much less works done with cyanates and isocyanates [2–4]. The most direct strategy of reacting organic halides with inorganic cyanates salts is also not a practical route for the synthesis of organic cyanates and isocyanates, but theoretical investigation can shed light on the detail of mechanism for the ion pair S_N2 reactions (Eq. (1)).

$$MNCO + RX \rightarrow RNCO \text{ or } ROCN \quad (1)$$

Comparing with the anionic S_N2 reactions, the ion pair S_N2 reactions have been less studied from the theoretical work even though some experiments results are known [5–10]. Pioneer research of Harder et al. [11] reported theoretical studies on some identity ion pair S_N2 reactions at carbon $MX + CH_3X$ (M=Li, Na; X=F, Cl) at the level of MP4/6-31+G*//HF/6-31+G*. Streitwieser et al. [12] extended the work to the higher alkyls with RHF, MP2, and B3LYP methods with 6-31+G* and discussed some steric effects for the ion pair displacement reactions. Leung and Streitwieser [13] investigated the structure of lithium and sodium cyanates and their related monomeric ion pair, and dimeric ion pair S_N2 reactions with methyl halides, $Y + CH_3X$ [Y=MNCO, MOCN, $(MNCO)_2$ (M=Li and Na); X=F, Cl]. Their calculated results show that methyl cyanate should form preferentially on analyses of transition structures if the reaction involves a monomer ion pair inversion pathway. More recently, Ren et al. [14] reported the higher G2M(+) level calculations for the identity ion pair S_N2 reactions at nitrogen $LiX + NH_2X$ and at carbon $LiX + CH_3X$ (X=F–I) [15]. All of above theoretical studies indicate that the ion pair S_N2 reaction involves preliminary encounter dipole–dipole complex instead of a negatively charged ion–dipole complex in the anionic S_N2 reactions, then proceeds via a cyclic transition structure.

* Corresponding author. Tel.: +86 28 85412800; fax: +86 28 85257397
E-mail address: yiren57@hotmail.com (Y. Ren).

0166-1280/$ - see front matter © 2004 Elsevier B.V. All rights reserved.
doi:10.1016/j.theochem.2004.08.020

Glukhovtsev et al. [16] pointed out that the anionic S_N2 reaction of CH_3X with X^- can, at least in principle, take place by either backside or front side attack, leading to displacement products with inversion or retention of configuration, though the barrier for the front attack is significantly higher. Interestingly, the two reaction mechanisms, inversion and retention, involved in the ion pair S_N2 reactions are competitive with each other. Our previous theoretical studies on the ion pair S_N2 reactions $LiY + CH_3X$ (Y, X = F, Cl, Br, and I) with inversion and retention mechanisms showed that the retention mechanism is favorable for all of the reactions involving fluorine [17].

The aim of present work is to contribute to a better understanding of the ion pair S_N2 reaction at carbon and to clarify the nature of all possible transition states. We will explore the retention mechanism for the reaction $LiNCO + CH_3F$ (Eq. (2)) and hope to address what is the most possible pathway. Meanwhile the entropy and solvent effects were considered here because these effects might produce the significant influence on the reaction and lead to different products. For comparing, the inversion mechanism was also studied at the same level of theory.

$$LiNCO + CH_3X \rightarrow CH_3NCO \text{ or } CH_3OCN \quad (2)$$

2. Methodology

All geometries were fully optimized at the level of HF/6-31+G** in the gas phase. The electron correlation effect was taken into account by further single point MP2 calculation with all electron being included in the correlation treatment, i.e. MP2(full)/6-31+G**//HF/6-31+G**, hereafter denoted as MP2(full). All stationary points were characterized by normal mode analysis at the HF/6-31+G** level and scaled vibrational zero-point energies (ZVPE) by a factor of 0.9 [18] were included in the calculations of relative MP2(full) energies. Atomic charges were calculated by use of the Natural Population Analysis (NPA) [19] at the MP2(full) level. The solvent effects on the title reaction (Eq. (2)) have been considered with a polar solvent CH_3COCH_3 ($\varepsilon = 20.70$) and a nonpolar solvent CCl_4 ($\varepsilon = 2.228$). A polarized continuum model (PCM) [20] was used for optimization at the HF/6-31+G** level. All calculations were performed using GAUSSIAN 98 system of program [21].

Throughout this paper, all inter-nuclear distances are in Å and bond angles are in deg. All relative energies in kcal/mol within the text were evaluated by the Gibbs free energy changes, ΔG_{298}, at 298.15 K. Calculated total Gibbs free energies, G_{298}(gas), dipole moments, μ(g), in the gas phase and the solvent stabilization energies, SSE, for all species in the title reaction (Eq. (2)) are listed in Table 1.

3. Results and discussion

3.1. Reactants

The predicted main geometries of lithium cyanate are shown in Fig. 1. There are two possible lithium cyanate isomers, LiNCO (**2a**) and LiOCN (**2b**), in which **2a** is the minimum energy form. Our calculations in the gas phase indicate that **2a** is 13.28 kcal/mol more stable than **2b**. The equilibrium isomerization barrier is 15.15 kcal/mol at the level of MP2(full). The T-shape π-complex structure is another isomer of lithium cyanate and a little bit stable than linear LiOCN at the level of MP2/6-31G** [22], but

Table 1
Calculated total Gibbs free energies (hartree), G_{298}(gas), dipole moments (D), μ(g), in the gas phase and the solvent stabilization energies (kcal/mol), SSE, for reactants, products, and transition structures in the ion pair S_N2 reaction $LiNCO + CH_3F$

	HF/6-31+G**	MP2(full)/6-31+G**//HF/6-31+G**			
	G_{298}(gas)	G_{298}(gas)	μ(g)	SSE[a]	SSE[b]
CH_3F (**1**)	−139.032707	−139.367822	2.19	−0.78	0.48
LiNCO (**2a**)	−174.707307	−175.193837	9.32	−18.59	−7.49
LiOCN (**2b**)	−174.686272	−175.172673	11.45	−24.14	−10.26
iso-TS	−174.680146	−175.169698	6.43	−19.14	−7.41
inv-TS1 (**3a**)	−313.659318	−314.491444	2.00	−8.33	−1.75
inv-TS2 (**3b**)	−313.657627	−314.490972	2.65	−9.31	−2.19
inv-TS3 (**3c**)	−313.629546	−314.449002	6.50	−15.70	−4.89
inv-TS4 (**3d**)	−313.648045	−314.471438	4.16	−10.30	−2.31
ret-TS1 (**3a′**)	−313.654396	−314.478560	5.86	−9.65	−2.30
ret-TS2 (**3b′**)	−313.655664	−314.478515	4.96	−9.14	−1.95
ret-TS3 (**3c′**)	−313.646595	−314.472860	4.87	−12.94	−3.74
ret-TS4 (**3d′**)	−313.661146	−314.487397	3.79	−9.18	−1.91
CH_3OCN (**4a**)	−206.780227	−207.407190	4.87	−4.08	−1.06
CH_3NCO (**4b**)	−206.739588	−207.361696	3.57	−2.75	−0.56
LiF (**5**)	−106.963848	−107.168790	6.65	−18.06	−7.56

[a] With HF/6-31+G** optimized geometries in polar solvent CH_3COCH_3($\varepsilon = 20.70$) solution.
[b] With HF/6-31+G** optimized geometries in nonpolar solvent CCl_4($\varepsilon = 2.228$) solution.

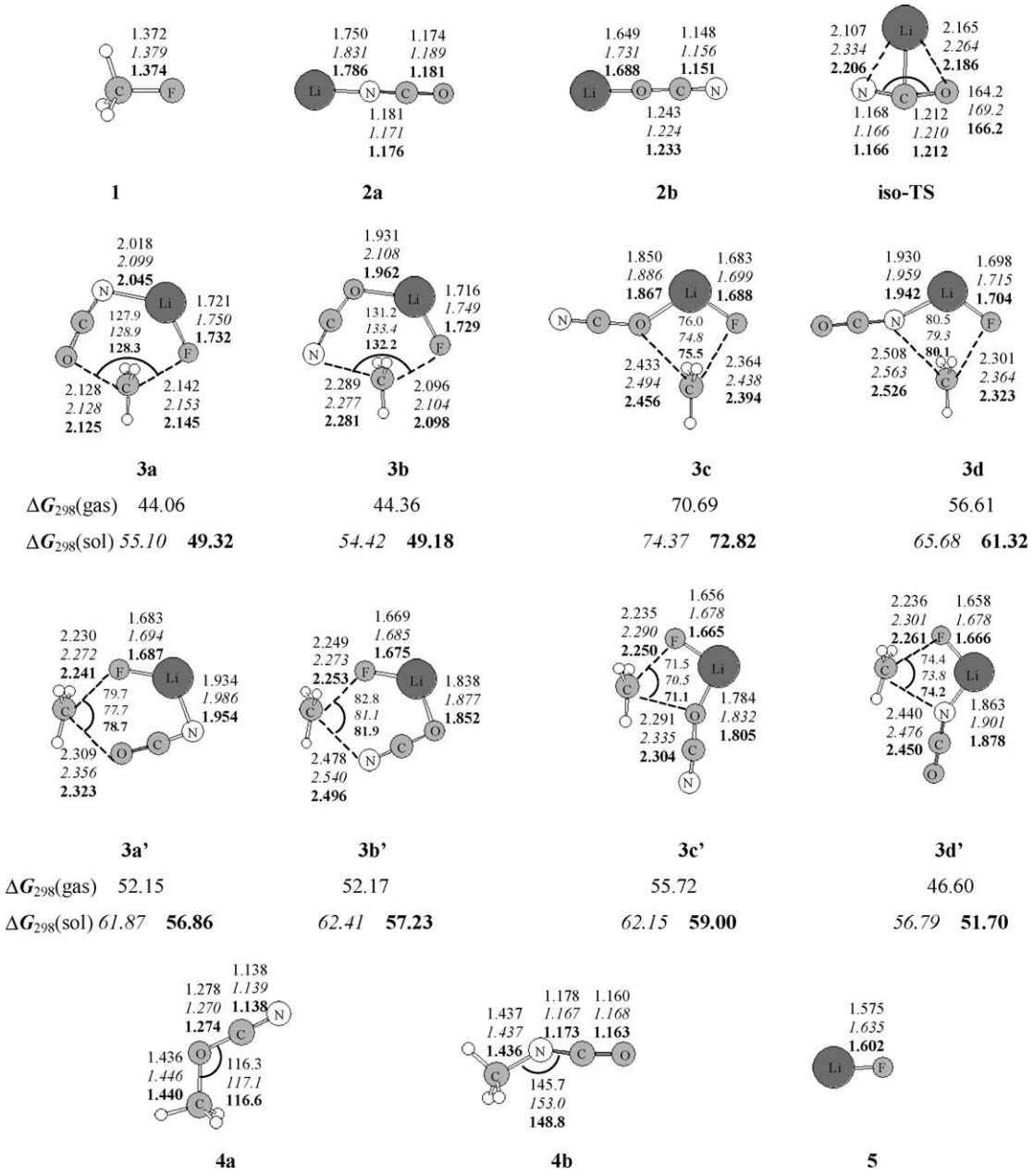

Fig. 1. Selected HF/6-31+G** optimized geometries of all species involved in the reaction LiNCO+CH_3F and the relative energies of transition states (ΔG_{298}) with respect to the minimum energy form of the separated reactants at the level of MP2(full)/6-31+G**//HF/6-31+G**+ZPE in the gas phase (in regular font), in CH_3COCH_3 (in italic) and in CCl_4 (in bold), respectively.

the T-shape structure is a transition state (iso-TS) on the isomerization of LiNCO to LiOCN in the present work.

3.2. Products

Calculated geometrical parameters of two main products—methyl cyanate (**4a**) and methyl isocyanate (**4b**)—are shown in Fig. 1. At the HF/6-31+G** level, **4a** has a bent structure at the oxygen atom and the C–O–C angle is 116.3°, **4b** is not linear, the C–N–C angle is 145.7° and the N–C–O angle is 175.3°. **4b** was found to be 28.55 kcal/mol more stable than **4a**.

3.3. Transition state structures

Four different transition structures were found for the reaction LiNCO+CH_3F with inversion mechanism. Two of them (**3a**–**b**) involve a planar six-membered ring structure. The remaining two (**3c**–**d**) are planar four-membered ring structures. Other four TS structures, **3a′**–**d′**, were located if the reaction follow the retention mechanism. In these retention TS structures, the nucleophilic site attacks methyl fluoride from front side of central carbon atom and leaving group and nucleophile are on the same side of CH_3 moiety. One nucleophilic site (N) of the isothiocyanate coordinates

with lithium, and the other nucleophilic site (O) attacks methyl fluoride, leading to a six-membered ring TS structure (**3a′**). In another six-membered ring TS structure **3b′**, the nucleophilic site (O) of the cyanate coordinates with lithium and the other nucleophilic site (N) attacks methyl fluoride. If the same oxygen atom (N) on the LiNCO moiety or nitrogen atom (O) on the LiOCN moiety coordinates with lithium and attacks methyl fluoride from front side simultaneously, a four-membered ring TS structure (**3c′** or **3d′**) is formed.

In the six-membered ring retention TS structures, the bridging action of the lithium cation causes **3a′** and **3b′** remarkable deformations relative to the inversion TS geometries (**3a** and **3b**), the O–C–F or N–C–F angles decreasing from ∼130 to ∼80°. These geometric characteristics will increase the repulsion between nucleophilic site and the leaving group and destabilize the retention TS structures **3a′** and **3b′**. But in the four-membered ring inversion transition structures (**3c–d**) and the retention transition structures (**3c′–d′**), the O–C–F or N–C–F angles are almost same (∼80°). Retention TS structures (**3c′–d′**) are lower in energy than **3c** and **3d**, respectively. These phenomena may be attributed to the shorter C–F and Li–F distances, thus stabilize these retention TS structures and lower the reaction barrier.

The calculated reaction barriers for the title reaction relative to minimum form of reactants increase in the following order, 44.06(**3a**) < 44.36(**3b**) < 46.60(**3d′**) < 52.15(**3a′**)–52.17(**3b′**) < 55.72(**3c′**) < 56.61(**3d**) < 70.69 kcal/mol (**3c**), that indicates that **3a** is clearly the best transition structure and methyl cyanate should be the initial product in the gas phase reaction of LiNCO + CH_3F with inversion mechanism. On the other hand, the initial product will be methyl isocyanate if the ion pair reaction involves the retention mechanism.

3.4. Charge distributions

The geometrical characteristics of transition states and the reaction barriers can be further investigated by a study of charge distributions based on the 'natural charges' (NPA) of Reed and Weinhold [19]. The results are summarized in Table 2 for the inversion transition structures, **3a–d**, and in Table 3 for the retention transition structures, **3a′–d′**. Tables 2 and 3 also include the total 'group charges' on the methyl group by adding the contributions of the component atoms.

Table 2
MP2 natural population (NPA) charges of the inversion transition structures

Atom	3a	3b	3c	3d
C1[a]	0.036	−0.005	0.206	0.162
H	0.227	0.236	0.192	0.192
H	0.249	0.247	0.254	0.255
H	0.249	0.247	0.254	0.255
F	−0.885	−0.872	−0.936	−0.919
Li	0.955	0.961	0.963	0.955
N	−0.860	−0.882	−0.993	−1.120
C2[b]	0.793	0.794	0.689	0.927
O	−0.765	−0.726	−0.629	−0.706
CH_3[c]	0.762	0.724	0.906	0.863

[a] On the CH_3 moiety.
[b] On the NCO moiety.
[c] Group charge obtained by summing component carbon (C1) and hydrogens.

Table 3
MP2 natural population (NPA) charges of the retention transition structures

Atom	3a′	3b′	3c′	3d′
C1[a]	0.121	0.113	0.099	0.093
H	0.234	0.248	0.238	0.237
H	0.237	0.232	0.229	0.230
H	0.249	0.244	0.258	0.258
F	−0.907	−0.915	−0.905	−0.901
Li	0.958	0.966	0.970	0.958
N	−0.888	−0.813	−0.617	−1.094
C2[b]	0.819	0.813	0.673	0.924
O	−0.823	−0.887	−0.945	−0.707
CH_3[c]	0.841	0.836	0.824	0.819

[a] On the CH_3 moiety.
[b] On the NCO moiety.
[c] Group charge obtained by summing component carbon (C1) and hydrogens.

The NPA for all TS structures reveal considerable positive charges (+0.724 to +0.906) on the methyl groups, which suggests the organic moiety has typical carbocation character. So the ion pair S_N2 transition states can be modeled as an anion, $FLiNCO^-$ or $FLiOCN^-$, interacting with a methyl cation.

Charge distributions in Tables 2 and 3 also show that the leaving fluorine atom bears lower negative charge in **3a** (−0.885) and **3b** (−0.872), but high negative charge in **3c** (−0.936) and **3d** (−0.919), respectively. These charges on F atom can be related with the S_N2 reaction barriers. Generally speaking, in the S_N2 reaction, the more electrons

Table 4
The relative energies in the gas phase and in solution (kcal/mol), ΔG_{298}, with respect to the minimum energy form of the separated reactants at 298.15 K for the ion pair S_N2 reaction LiNCO + CH_3F

Pathway	Reactants	inv-TS[a]	ret-TS[b]	Products	Products
I or **V**	0.0[c]	44.06	52.15	19.56	CH_3OCN +
	0.0[d]	*55.10*	*61.87*	*16.79*	LiF
	0.0[e]	**49.32**	**56.86**	**17.95**	
II or **VI**	0.0	44.36	52.17	−8.99	CH_3NCO +
	0.0	*54.42*	*62.41*	*−10.42*	LiF
	0.0	**49.18**	**57.23**	**−10.09**	
III or **VII**	0.0	70.69	55.72	19.56	CH_3OCN +
	0.0	*74.37*	*62.15*	*16.79*	LiF
	0.0	**72.82**	**59.00**	**17.95**	
IV or **VIII**	0.0	56.61	46.60	−8.99	CH_3NCO +
	0.0	*65.68*	*56.79*	*−10.42*	LiF
	0.0	**61.32**	**51.70**	**−10.09**	

[a] Pathways (**I–IV**) via inv-TS.
[b] Pathways (**VI–VIII**) via ret-TS.
[c] Relative free energies in the gas phase.
[d] Relative free energies in polar solvent CH_3COCH_3 (ε = 20.70).
[e] Relative free energies in nonpolar solvent CCl_4 (ε = 2.228).

on the same leaving group, the later transition state, the higher the reaction barrier, that is consistent with the results in Table 4. The barriers for reaction pathways via **3c** (70.69 kcal/mol) or **3d** (56.61 kcal/mol) are higher than others. The charges on F atom in **3a′**–**d′** (−0.901 to −0.915) are between **3a**–**b** and **3c**–**d**, so the corresponding relative energies for **3a′**–**d′** (46.60–55.72 kcal/mol) are higher than **3a**–**b**, lower than **3c**–**d**.

3.5. Solvation effects

As shown in Fig. 1, the main modifications of the geometrical parameters induced by the solvents CH_3COCH_3 and CCl_4 are the lengthening of the Li–N and Li–O bonds in reactants and Li–F bond, which leads to the looser transition states in solution. Another significant solvent effects are the increase of angle C–N–C in CH_3NCO from 145.7 to 153.0° in CH_3COCH_3 and to 148.8° in CCl_4. Other geometries are influenced very little by the solvation effects.

Solvent effects on the total Gibbs free energies for all species, kinetic, and thermodynamic parameters for the title reaction are compiled in Tables 1 and 4, respectively. The relative Gibbs free energies in solution were computed by

$$\Delta G_{298}(\text{sol}) = \Delta G_{298}(\text{gas}) + \Delta\text{SSE}$$

These data show that the energy gaps between LiNCO and LiOCN are reduced from 13.28 kcal/mol in the gas phase to 7.73 kcal/mol in CH_3COCH_3 and 10.51 kcal/mol in CCl_4, respectively, due to LiOCN with larger dipole moment (11.45 D) than LiNCO (9.32 D). The reaction of LiNCO + CH_3F will be retarded in solution, which might be taken as a reflection of stronger solvation of the free reactants relative to the transition structures. LiNCO and LiOCN have dipole moments of 9.32 D and 11.45 D, respectively, while TS structures have smaller dipole moments of less than 6.50 D in the gas phase. The decrease in dipole moment accompanying this reaction course implies that a polar solvent should be able to retard the reaction more than a nonpolar solvent. The reaction barriers in polar solution CH_3COCH_3 are higher than those in the gas phase, increasing in the order: 54.42(**3b**) < 55.10(**3a**) < 56.79(**3d′**) < 61.87(**3a′**) < 62.15(**3c′**) < 62.41(**3b′**) < 65.68(**3d**) < 74.37 kcal/mol (**3c**). The barriers in nonpolar solvent are lower than those in polar solvent, but follow the same order for the four transition structures with lower energies: 49.18(**3b**) < 49.32(**3a**) < 51.70(**3d′**) < 56.86(**3a′**). The most intriguing point is that **3b** is more stable than **3a** by 0.68 kcal/mol in CH_3COCH_3 or 0.14 kcal/mol in CCl_4. So, the thermodynamically favorable CH_3NCO will be the product if the reaction LiNCO with CH_3F occurs in solution, which can be explained by the larger dipole moment of **3b** (2.65 D) than **3a** (2.00 D).

3.6. Exploring reaction pathways

It is obvious that there are following eight possible reaction pathways, in which **I**–**IV** proceed via the inversion mechanism, while **V**–**VIII** by the retention mechanism.

$$\text{I}: \ \text{LiNCO(2a)} + \text{CH}_3\text{F} \rightarrow \text{inv} - \text{TS1(3a)} \rightarrow \text{CH}_3\text{OCN(4a)} + \text{LiF}$$

$$\text{II}: \ \text{LiNCO(2a)} \rightarrow \text{LiOCN(2b)}$$

$$\text{LiOCN(2b)} + \text{CH}_3\text{F} \rightarrow \text{inv} - \text{TS2(3b)} \rightarrow \text{CH}_3\text{NCO(4b)} + \text{LiF}$$

$$\text{III}: \ \text{LiNCO(2a)} \rightarrow \text{LiOCN(2b)}$$

$$\text{LiOCN(2b)} + \text{CH}_3\text{F} \rightarrow \text{inv} - \text{TS3(3c)} \rightarrow \text{CH}_3\text{OCN(4a)} + \text{LiF}$$

$$\text{IV}: \ \text{LiNCO(2a)} + \text{CH}_3\text{F} \rightarrow \text{inv} - \text{TS4(3d)} \rightarrow \text{CH}_3\text{NCO(4b)} + \text{LiF}$$

$$\text{V}: \ \text{LiNCO(2a)} + \text{CH}_3\text{F} \rightarrow \text{ret} - \text{TS1(3a}\prime\text{)} \rightarrow \text{CH}_3\text{OCN(4a)} + \text{LiF}$$

$$\text{VI}: \ \text{LiNCO(2a)} \rightarrow \text{LiOCN(2b)}$$

$$\text{LiOCN(2b)} + \text{CH}_3\text{F} \rightarrow \text{ret} - \text{TS2(3b}\prime\text{)} \rightarrow \text{CH}_3\text{NCO(4b)} + \text{LiF}$$

$$\text{VII}: \ \text{LiNCO(2a)} \rightarrow \text{LiOCN(2b)}$$

$$\text{LiOCN(2b)} + \text{CH}_3\text{F} \rightarrow \text{ret} - \text{TS3(3c}\prime\text{)} \rightarrow \text{CH}_3\text{OCN(4a)} + \text{LiF}$$

$$\text{VIII}: \ \text{LiNCO(2a)} + \text{CH}_3\text{F} \rightarrow \text{ret} - \text{TS4(3d}\prime\text{)} \rightarrow \text{CH}_3\text{NCO(4b)} + \text{LiF}$$

The pathways (**I** and **II**) involving six-membered ring inversion TS structure are more favorable in the gas phase and in solution. The most possible pathway in the gas phase is **I**, passing through TS (**3a**) to reach the initial product CH_3OCN (**4a**). But the predicted pathway in solution is different that will start from the isomerization of lithium isocyanate to lithium cyanate and proceed via the saddle point (**3b**), forming the more stable product CH_3NCO (**4b**).

4. Conclusions

Application of MP2(full) theory to the ion pair S_N2 reaction of lithium isocyanates with methyl fluoride in the gas phase and in solution leads to the following conclusions:

(1) For the ion pair S_N2 reaction $LiNCS + CH_3F$ with inversion and retention mechanism, eight possible reaction pathways (**I–VIII**) are predicted.
(2) The six-membered ring inversion transition structures (**3a** and **3b**) are much lower in energy than others (**3c** and **3d**) and methyl cyanate should form preferentially in the gas phase if the reaction involves inversion mechanism.
(3) The four-membered ring retention transition structure (**3d′**) is more stable than other TS structures (**3a′–c′**) and methyl isocyanate will be the initial product in the gas phase if the reaction follows retention mechanism.
(4) Solvent effects will retard the rate of title reaction and change the reaction pathway. More stable methyl isocyanate will be product in solution based on the analyses of kinetic and thermodynamic investigations.
(5) Comparison between two mechanisms shows that inversion mechanism is more favorable no matter in the gas phase or in solution.

Acknowledgments

H.-J. Zhu acknowledges the support of 'Bairenjihua' Fund from CAS. Y. Ren is thankful for the support from the Scientific Research Foundation for the Returned Chinese Scholars of Sichuan University.

References

[1] S. Patai (Ed.), The Chemistry of Cyanates and Their Thio Derivatives, Wiley, New York, 1977.
[2] D. Poppinger, L. Radom, J. Am. Chem. Soc. 100 (1978) 3674.
[3] M.A. McAllister, T.A. Tidwell, J. Chem. Soc. Perkin Trans. 2 (1994); 2239.
[4] P.W. Schultz, G.E. Leroi, J.F. Harrison, Mol. Phys. 88 (1996) 217.
[5] S. Winstein, L.G. Savedoff, S. Smith, I.D.R. Stevens, J.S. Gall, Tetrahedron Lett. 1960; 24.
[6] P. Cayzergues, C. Georgoulis, G. Mathieu, J. Chim. Phys. Phys. Chim. Biol. 84 (1987) 63.
[7] K.C. Westaway, Z. Waszczylo, P.J. Smith, K.S. Rangappa, Tetrahedron Lett. 26 (1985) 25.
[8] K.C. Westaway, Z.-G. Lai, Can. J. Chem. 66 (1988) 1263.
[9] K.C. Westaway, Z.-G. Lai, Can. J. Chem. 67 (1989) 345.
[10] Z.-G. Lai, K.C. Westaway, Can. J. Chem. 67 (1989) 21.
[11] S. Harder, A. Streitwieser, J.T. Petty, P.v.R. Schleyer, J. Am. Chem. Soc. 117 (1995) 3253.
[12] A. Streitwieser, G.S.-C. Choy, F. Abu-Hasanayn, J. Am. Chem. Soc. 119 (1997) 5013.
[13] S.S.W. Leung, A. Streitwieser, J. Comput. Chem. 19 (1998) 1325.
[14] Y. Ren, S.-Y. Chu, Chem. Phys. Lett. 376 (2003) 524.
[15] Y. Ren, S.-Y. Chu, J. Comput. Chem. 25 (2004) 461.
[16] M.N. Glukhovtsev, A. Pross, H.B. Schlegel, R.D. Bach, L. Radom, J. Am. Chem. Soc. 118 (1996) 11258.
[17] Y. Xiong, H.-J. Zhu, Y. Ren, J. Mol. Struct. (Theochem) 664–665 (2003) 279.
[18] A.P. Scott, L. Radom, J. Phys. Chem. 100 (1996) 16502.
[19] A.E. Reed, R.B. Weinstock, F. Weinhold, J. Chem. Phys. 83 (1985) 735.
[20] J. Tomasi, M. Persico, Chem. Rev. 94 (1994) 2027.
[21] M.J. Frisch, G.W. Trucks, H.B. Schlegel, et al., GAUSSIAN 98, Revision A.9, Gaussian, Inc., Pittsburgh, PA, 1998.
[22] T. Veszprémi, T. Pasinszki, M. Feher, J. Am. Chem. Soc. 116 (1994) 6303.